



Distributed wide field electromagnetic method based on high-order 2^n sequence pseudo random signal

Yang YANG¹, Ji-shan HE^{2,3}, Fan LING^{2,3}, Yu-zhen ZHU^{1,4}

1. Geotechnical and Structural Engineering Research Center, Shandong University, Ji'nan 250061, China;
2. Institute of Urban Underground Space and Energy Studies, The Chinese University of HongKong, Shenzhen 518172, China;
3. School of Geosciences and Info-Physics, Central South University, Changsha 410083, China;
4. Shandong Coal Geological Planning and Exploration Research Institute, Ji'nan 250109, China

Received 30 September 2021; accepted 22 February 2022

Abstract: To make three-dimensional electromagnetic exploration achievable, the distributed wide field electromagnetic method (WFEM) based on the high-order 2^n sequence pseudo-random signal is proposed and realized. In this method, only one set of high-order pseudo-random waveforms, which contains all target frequencies, is needed. Based on high-order sequence pseudo-random signal construction algorithm, the waveform can be customized according to different exploration tasks. And the receivers are independent with each other and dynamically adjust the acquisition parameters according to different requirements. A field test in the deep iron ore of Qihe–Yucheng showed that the distributed WFEM based on high-order pseudo-random signal realizes the high-efficiency acquisition of massive electromagnetic data in quite a short time. Compared with traditional controlled-source electromagnetic methods, the distributed WFEM is much more efficient. Distributed WFEM can be applied to the large scale and high-resolution exploration for deep resources and minerals.

Key words: distributed wide field electromagnetic method (WFEM); high-order pseudo-random signal; multi-frequency; massive data

1 Introduction

Wide field electromagnetic method (WFEM) is a widely used frequency-domain electromagnetic exploration method with controlled sources. Since a complete and non-approximate electromagnetic field calculation formula is applied, a large exploration depth can be obtained under the condition of a small transmission and reception distance [1–4]. Moreover, only one component is needed in actual exploration, which makes the field work greatly simplified. Benefitted from the application of 2^n sequence pseudo-random signals for exploration, the simultaneous transmission and

reception of multiple frequencies is realized [5,6]. With the same acquisition time, more frequencies are obtained in WFEM, and the exploration efficiency is greatly improved. Based on the above characteristics, WFEM has been widely used in the exploration of deep oil and gas, unconventional oil and gas, metal minerals, geological disasters, and urban underground space, and has obtained good detection results [7–12].

The use of 2^n sequence pseudo-random signal is an important improvement for electromagnetic exploration. In fact, there are many types of electromagnetic prospecting signals for different electromagnetic methods, and different types of prospecting signals have their own advantages and

characteristics [13–18]. However, some signal types are not suitable for frequency domain exploration. 2^n sequence pseudo-random signal based on the self-closing method of $-1, 0, 1$ is first constructed in the 1990s [6]. Its main frequencies are evenly distributed in the logarithm frequency domain, and the energy of each main frequency is relatively uniform, which is quite suitable for frequency electromagnetic exploration. Benefitted from 2^n sequence pseudo random signal, multiple frequencies are simultaneously transmitted and acquired at the same time. This has brought huge advantages for later data processing, especially in strong interference environments.

At present, in the real exploration of WFEM, the transmission is mainly based on the 2^n pseudo random signal in Type 7, that is, there are 7 main frequencies in it. If 40 or more frequencies are to be obtained, under normal circumstances, only 6 frequency groups need to be changed for transmitting. Traditionally, in order to distinguish the waveforms, these 6 frequency groups are defined as Types 7-0, 7-1, 7-2, 7-3, 7-4 and 7-5. Type 7-0 corresponds to 128, 256, 512, \dots , 8192 Hz, 7-2 corresponds to 1, 2, 4, \dots , 64 Hz, 7-4 corresponds to 0.015625, 0.03125, 0.0625, \dots , 1 Hz, and 7-3 corresponds to transmission frequency of 1.5, 3, 6, \dots , 96 Hz, as encrypted frequency group of 7-2. Types 7-1 and 7-5 are the encrypted frequency groups of 7-0 and 7-4, respectively [2]. Different versions of instrument may have different naming methods, but the naming principles are the same.

However, the continuous development of industry puts forward higher requirements for electromagnetic prospecting. On the one hand, the demand for large-scale and high-resolution exploration is increasing, and the demand for short-term and large-scale exploration is even stronger. Seismic exploration methods have realized distributed, node-type 3D exploration. In contrast, the development of distributed 3D electromagnetic exploration is relatively slow. On the other hand, the surrounding environment of the electromagnetic survey becomes more and more complex, such as exploration in mining areas, cities, and surrounding areas. Due to factors such as acquisition time and noise interference, the exploration data often have a poor signal-to-noise ratio, and many algorithms have been proposed to cope with that [19–22].

When conducting exploration in a mining area, interference often requires the multi-period collection to suppress, but the time for data acquisition is often limited. In the same survey area, interference in some locations is extremely strong, while the noise in other locations is relatively weak. The unified acquisition parameters need to be adjusted according to different situations. How to obtain more exploration data with a high signal-to-noise ratio under the circumstance of limited acquisition time and widespread noise interference is an urgent problem to deal with.

In this work, based on the traditional WFEM, a faster and more efficient acquisition method is proposed, to realize distributed WFEM by designing and transmitting high-order pseudo-random signals. Its main feature is that only one set of high-order pseudo-random signals, which contains all target frequencies, is needed in exploration. In addition, multi-channel distributed WFEM receiving terminals are used for blind acquisition, which fully increases the degree of freedom of electromagnetic data acquisition. It truly realizes independent acquisition and dynamically adjusts the signal acquisition time according to the actual noise situation in different locations. Then, through technical means such as denoising and harmonic extraction, the effective components, including both main frequencies and harmonics, can be obtained to the maximum extent. Based on distributed WFEM, the acquisition of large-scale and massive electromagnetic data is realized.

2 High-order pseudo-random signal

2.1 Realization of high-order pseudo-random signal

The main feature of the distributed WFEM is the application of high-order 2^n sequence pseudo-random signals, and in that sense, only one set of waveforms needs to be sent during exploration. Therefore, how to design and select exploration signals has become the key to the realization of distributed WFEM. In the 1990s, a_k^n sequence pseudo-random signal based on self-enclosed addition was proposed [6]. Because of good spectrum characteristics, a_k^n sequence pseudo-random signal has been successfully applied to electromagnetic exploration and other electrical exploration [2]. 2^n signal is a special type of a_k^n

pseudo-random signal. The main frequencies of the 2ⁿ signal are increased by a multiple of 2 and equally logarithmic-distributed in the frequency domain. It needs to be noted that the 2ⁿ sequence signal is a signal not only for the WFEM and the induced polarization method but also in other scenarios.

In practical applications, the pseudo random signal in Type 7 is usually the mainstay. During exploration, it only needs to change the frequency group a few times to obtain the information for dozens of target frequencies. Figures 1(a, b) show the waveform and spectrum of the waveform in Type 7-2. The lowest frequency is 1 Hz, and the highest frequency is 64 Hz. The main frequency is increased by a multiple of 2, and there are 7 main frequencies in total, which is also the reason why it is called Type 7.

In real exploration, waveforms with more frequencies, such as waveforms in Type 11 and Type 15, as shown in Fig. 1(c, e), can also be applied according to the actual situation to cope with different exploration tasks. Whether it is Type 11 or 15, the main frequencies are increased by multiple of 2 and are evenly distributed.

In the past, if it is desired to further increase the exploration frequency, it was often achieved by sending an additional set of pseudo-random signals

with different fundamental frequencies, such as signal in Type 11 with a fundamental frequency of 1.5 Hz, to achieve encryption of the exploration frequency for signal in Type 11 with a fundamental frequency of 1 Hz.

In fact, in the 2ⁿ sequence pseudo-random signal, in addition to the main frequency components, many harmonics can also be applied, and the application of harmonics will help achieve the goal of sending only a set of waveforms to complete the exploration. To extract the effective frequency components of harmonics, a method of harmonic extraction and a method of the frequency density calculation are proposed [23]. By analyzing the theoretical waveforms and spectrum of the signal in Type 7 and Type 11 with time domain amplitude of 100 A, it can be found that there are indeed many harmonics with relatively large values, as shown in Figs. 2(a, b). There are 19 frequencies with amplitude larger than 10 A in Type 11, and 71 frequencies with amplitude larger than 5 A in Type 15, in which there both exist a lot of potential effective components.

But at the same time, the distribution of high-amplitude harmonics is not as uniform as the main frequency, as shown in the frequency density curve in the Figs. 2(c, d) [24]. There are more frequencies in some frequency bands than in other

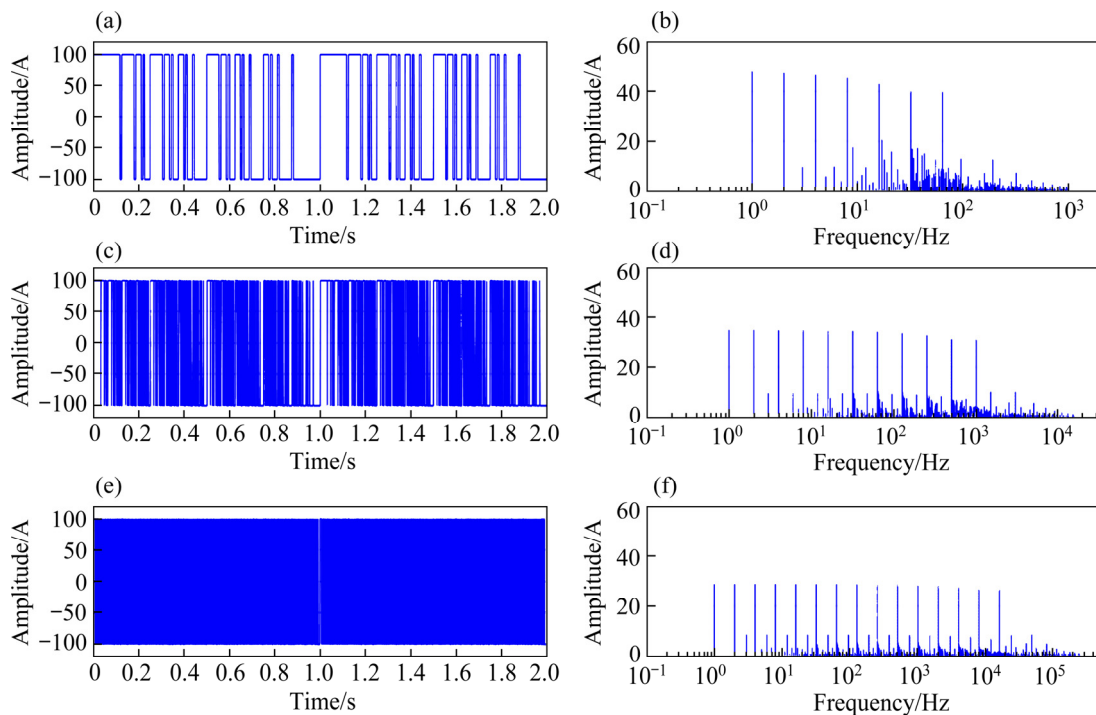


Fig. 1 Waveforms (a, c, e) and spectra (b, d, f) of typical 2ⁿ signal in different types: (a, b) Type 7-2; (c, d) Type 11; (e, f) Type 15

bands. The harmonic extraction method can indeed obtain more frequencies, but the effective frequency components obtained are not evenly distributed. Although the use of harmonics can increase the number of exploration frequencies in quantity, the frequencies cannot be customized according to needs. Therefore, only based on the extraction of harmonics, it is not possible to achieve the goal of exploration by sending one traditional pseudo random waveform.

In this context, based on the self-closing addition of 1, -1, and 0, considering parameters of

frequency displacement, amplitude and phase, the high-order 2^n sequence pseudo-random signal is constructed [25]. As shown in Figs. 3(a, b), the high-order pseudo random signal is the second-order 27-frequency wave, noted as Type L2-F27, in which L means level and F means main frequencies. It can be considered as the composition of one set of 15 frequencies of 0.25, 0.5, ..., 2048 Hz, and another set of 14 frequencies of 0.75, 1.5, ..., 3072 Hz. This is the reason why it is called a second-order 2^n sequence pseudo-random signal. As shown in Figs. 3(a, b), when the amplitude of the

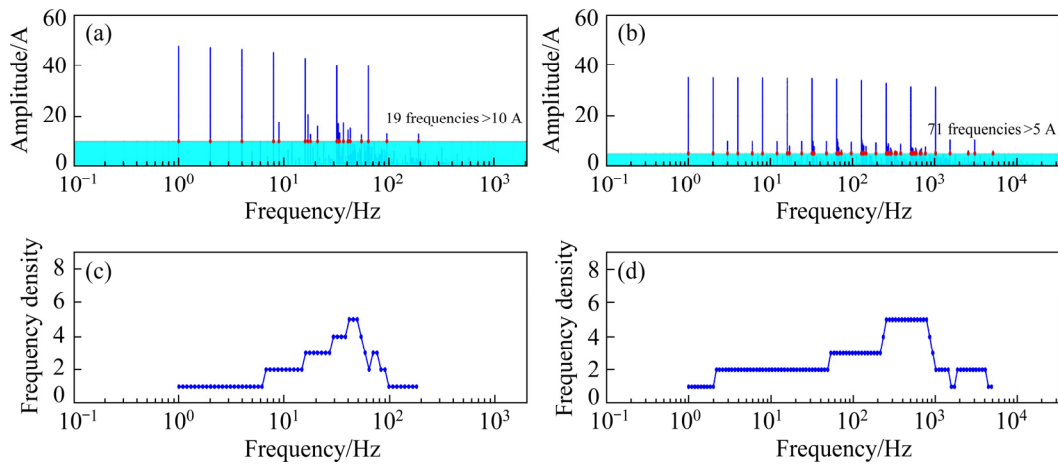


Fig. 2 Spectra of ideal waveform (a, b) and frequency density curves for signal (c, d) in Type 7-2 (a, c) and Type 11 (b, d)

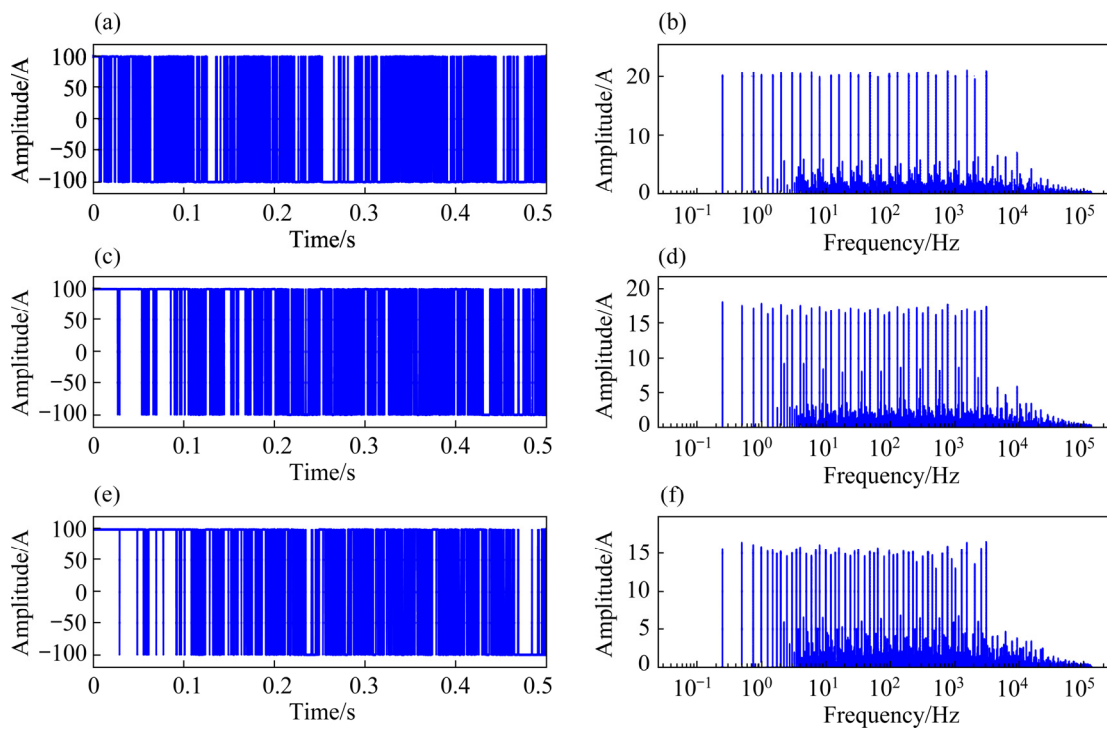


Fig. 3 Waveforms (a, c, e) and spectra of waveform (b, d, f) in Type L2-F27 (a, b), Type L3-F39 (c, d) and Type L4-F49 (e, f)

current in the time domain is 100 A, the average amplitude of its frequency components is larger than 20 A. Based on the same method, a third-order 39-frequency containing 39 dominant frequencies, noted as L3-F39, was constructed, as shown in Figs. 3(c, d), with an average amplitude larger than 17 A. The waveform and spectrum of the signal in Type L4-F49 are shown in Figs. 3(e, f), respectively, in which the average amplitude of the main frequency is about 15 A. It is obvious that the number of main frequencies corresponding to the typical signal in high order is odd. In this case, there are only 1, -1 in the signal and only 100 and -100 in the corresponding waveform. This is deliberately designed to prevent the instrument from being empty. In fact, when the number of main frequencies is even, there will be 1, 0, -1 in the signal.

Besides signal types above, a much higher order pseudo random signal in Type L6-F81 was also designed. Figures 4(a, b) show the waveform and spectrum of the ideal signal in Type L6-F81, respectively, with the lowest frequency of 0.0625 Hz and the highest frequency of 3072 Hz. The average amplitude of each frequency is larger than 10 A. The transmission test was successfully carried out in the field by an electrical source with a length of 1.35 km. Figures 4(c, d) show the waveform and spectrum of the real transmitted signal, respectively.

Affected by the earth, instrument, and long wires, the real transmitted waveform of the pseudo-random signal is a little different from the theoretical waveform, especially the high frequency components. Compared with the theoretical wave-

form, the current value corresponding to frequencies above 300 Hz is significantly reduced, but the overall signal still maintains good spectral characteristics. With the current about 120 A in the time domain, the amplitude of most of the main frequencies in the frequency domain is larger than 10 A, and some of the main frequencies even reach 15 A.

By comparing the spectrum of high-order pseudo-random signals of different orders, it is found that as the number of main frequencies increases, the average amplitude of the main frequency is decreased, but the rate of decrease gets slower. This is because the main frequency amplitude is not geometrically decreased, but roughly decays to the power of $-1/2$. This has been explained in detail by previous studies [24,26]. It is also noted that for high-order pseudo-random signals, as the order increases, the number of main frequencies in different frequency bands increases uniformly, and the main frequencies are relatively evenly distributed. And it is obvious that high-order pseudo-random signals can be also applied to other application scenarios.

At the same time, it is necessary to comprehensively consider hardware performance during real applications. Different hardware modules correspond to different performance conditions, and it is sure that not all design waveforms can be realized under limited hardware conditions. Therefore, when selecting the order and frequency components of a high-order pseudo-random signal, the exploration purpose and hardware conditions should be considered comprehensively.

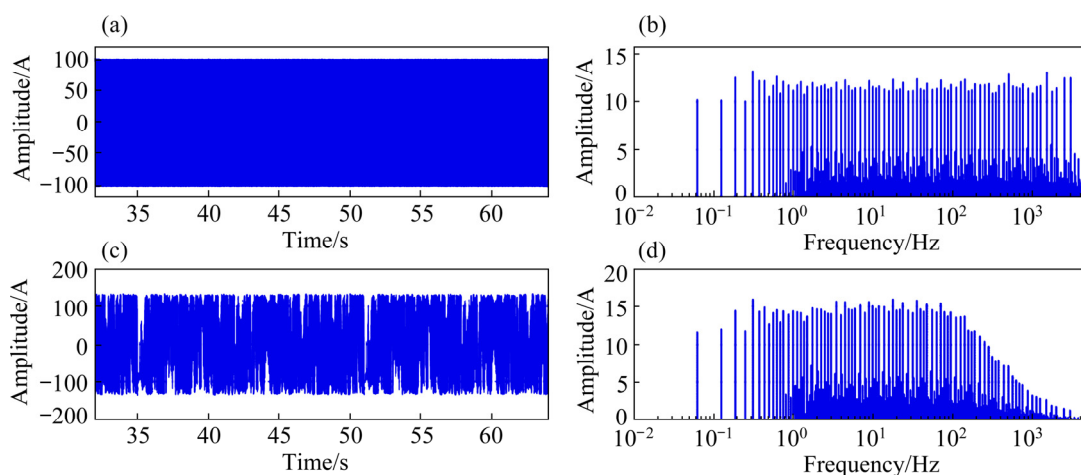


Fig. 4 Ideal waveform (a) and spectrum of ideal signal (b); waveform (c) and spectrum of real transmitted signal (d) in Type L6-F81

2.2 Characteristics of high-order pseudo-random signal

In the past, electromagnetic equipment, such as V8 and GDP32, obtained the information for all target frequencies through frequency sweeping mode, that is, only one frequency was sent at one time. The current in field work is generally 20–30 A. For high-order pseudo-random signals, taking waveform in Type L3-F39 (39-frequency wave) as an example, if this wave is transmitted using a 200 kW or higher power generator, the effective current can reach 120 A or higher in a real case. The average current of the main frequencies of 39-frequency wave is larger than 20 A, which is very close to the current of single-frequency emission based on traditional equipment. Furthermore, when frequency sweeping mode is applied to surveying, if the acquisition time of each frequency is 2 min, it will take 78 min to observe 39 frequencies in total. However, if the acquisition time for the 39-frequency wave is 78 min, the corresponding acquisition time for each frequency is 78 min too, which is 39 times the acquisition time of the frequency sweep mode. By using a high-order pseudo-random signal, the acquisition time of each frequency is longer in exploration. Thus, with the precondition of the same current, the signal-to-noise ratio of electromagnetic data based on high-order pseudo-random signals is much larger.

If the generator of the same power is used to send 39-frequency waves and single-frequency waves separately, the average amplitude of main frequencies in the 39-frequency wave is about $1/6.8$ of the corresponding amplitude of single-frequency transmission [24]. If acquisition time for each frequency is 2 min in frequency sweeping mode, the acquisition time of total 39 frequencies will be 78 min, while the acquisition time of each frequency in the case of 39-frequency wave is 78 min and 39 times that of a single frequency. In this case, if there exists Gaussian noise only in real data, the noise effect decreases by the $1/2$ power of the acquisition time based on central limit theorem [26]. In other words, if other conditions are unchanged, the Gaussian noise effect in 39-frequency wave becomes $1/\sqrt{39}$ of the effect in frequency sweep mode, which is about $1/6.25$. That is to say, for frequency sweeping mode, it has a larger amplitude, but less acquisition time. However, for 39-frequency wave, it has a smaller

amplitude, but much more acquisition time. Therefore, under the same transmission power and same total acquisition time, the signal-to-noise ratio of a single frequency and high-order pseudo-random signals is very close. However, it needs to be noted that the similar signal-to-noise ratio is under the condition of Gaussian noise only. In mining areas, complex urban environments, etc., various industrial and communication interferences and other non-Gaussian noises are ubiquitous. In that case, the signal-to-noise ratio is mainly affected by these noises rather than Gaussian noises. Non-Gaussian noises often have non-uniform characteristics in time distribution, that is, the noise intensity varies greatly at different moments. When observed with high-order pseudo-random signals, all frequencies are full-time acquisitions, making it easier to obtain useful data with a high signal-to-noise ratio through denoising methods [22].

Furthermore, in different noise conditions, for frequency sweeping mode, it often requires an appointment time for observation, and then the survey is conducted in sequence according to the target frequency table. However, the noise at different locations in the same area may vary greatly. It is possible that at some locations it does have very little noise and not need to be observed for a long time, while some other locations are quite noisy, requiring a longer acquisition time. Under such circumstances, it is unreasonable to use uniform acquisition parameters for all measuring points. When high-order pseudo-random signals are applied, data acquisition for receivers can be started at any time and stopped once the signal-to-noise ratio requirements are met. Further, there is no need for synchronization between receivers. For example, in some places with strong noise, the acquisition time can be increased for the higher signal-to-noise ratio, while in some places, when the noise is low, high-quality data can be obtained in a short time. Compared with the single frequency sweeping mode, when high-order pseudo-random signals are used, the acquisition time can be dynamically adjusted according to the noise situation to ensure the signal-to-noise ratio of different measuring points, making exploration more cost-effective.

3 Realization of distributed WFEM

Litun Iron Mine is in the northern part of

Qihe–Yucheng iron-rich ore comprehensive exploration area in Shandong Province, China. The iron ore in the area has the characteristics of large thickness, high grade, and great deep burial. The 900–1100 m shallows are Quaternary and Neogene, with low resistivity, 1100–1300 m shallows are Carboniferous, Permian strata, and the main surface has medium resistivity. The deep part is diorite, which is mainly characterized by high resistivity. There are mainly 5 boreholes in this area, as shown in Fig. 5, of which 4 meet ore and 1 meets mineralization. The ore depth is between 1100 and 1300 m, and the overall ore thickness is 58.78–119.67 m. The average ore grade is TFe 56.52% and mFe 51.65%. The ore body mainly exists in the contact zone with diorite and the Carboniferous–Permian, and it is a rich iron ore covering thick sedimentary strata. Besides, the area is with a quite flat surface, which is quite suitable for large-scale electromagnetic exploration.

Under such circumstances, the field test of distributed WFEM based on high-order pseudo-random signals was carried out. The survey area is equipped with 1350 survey points and 23 survey lines, as shown in Fig. 5. The bottom map gives the ground magnetic survey data. The blue point is the measurement point of WFEM. The survey line spacing is 100 m, part of the survey line spacing is 50 m, and the MN pole distance is 50 m. When conducting exploration, receiving terminal is equipped with 5 receiving groups, each of which controls 4 instruments, and each instrument has 5 acquisition channels, that is, one group controls 20 channels for acquisition, a total of 100 channels.

3.1 Field working method of distributed WFEM

Since high-order pseudo-random signal is applied in distributed WFEM, great changes have taken place in the way of WFEM observation, both in the transmitting terminal and receiving terminal, as shown in Fig. 6. Figure 6(a) shows the field working method of traditional WFEM and Fig. 6(b) shows the field working method of distributed WFEM.

3.1.1 Working method in transmitting terminal

In traditional WFEM, 6 frequency groups of waveforms are needed to transmit, and the total acquisition time for one routine is about 2 h, while in distributed WFEM, it only needs to transmit one waveform and the total acquisition time is about 0.5 h, since it only needs to count the lowest frequency acquisition time in distributed WFEM.

In a real application, the first thing is to select the frequency range based on the target detection depth and select the order of pseudo-random signal according to the resolution requirements, since only one set of waveforms is needed in distributed WFEM. A signal in Type L3-F39 is designed, of which the lowest frequency is 0.25 Hz, and the highest frequency is 3072 Hz. However, the target detection depth of Qihe–Yucheng is larger than 2000 m, and the main mineralization depth is 1100–1300 m. Besides, the thickness of the four series with low resistivity is about 900 m. Therefore, by a transformation, a new set of waveforms in Type L3-F39 was designed, in which the lowest frequency becomes 0.0625 Hz and the highest frequency is 768 Hz. The spectrum of the ideal transmitting signal is just like the spectrum shown in Fig. 6(b).

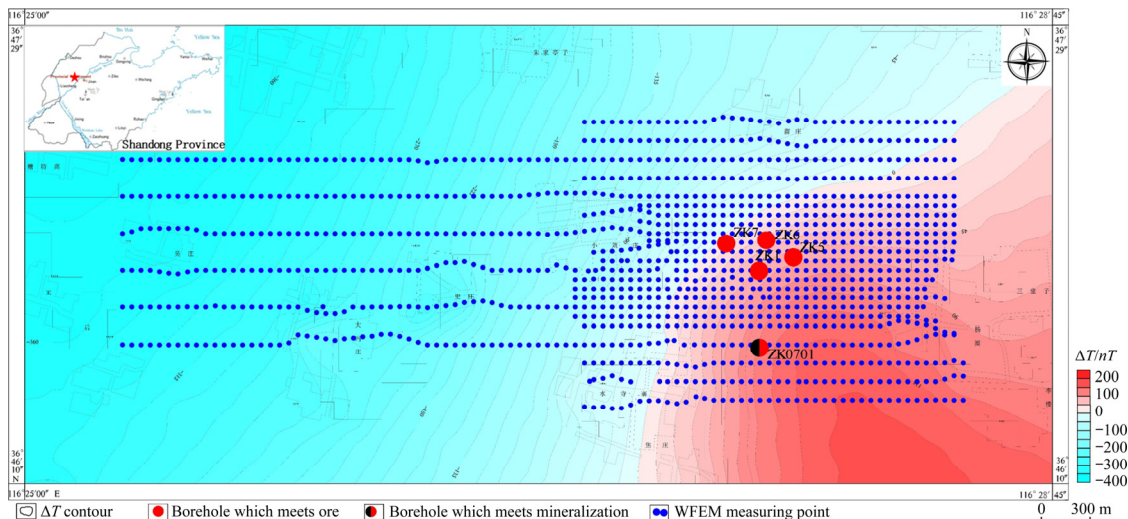


Fig. 5 Distribution of WFEM measurement points in Litun Iron Mine

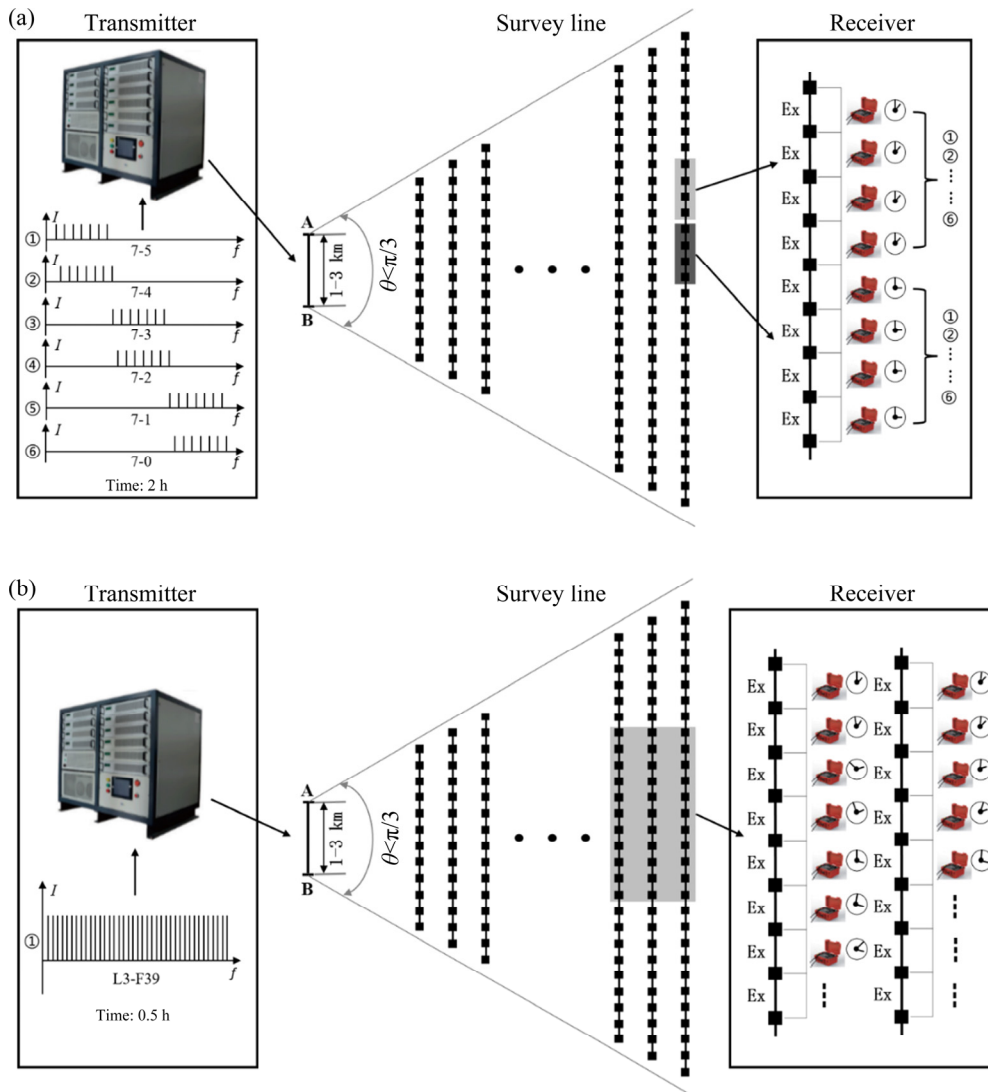


Fig. 6 Field working method for traditional WFEM (a) and distributed WFEM (b)

Based on an electrical source with a length of 1.5 km, the signal in Type L3-F39 is transmitted. And the transmission and reception distance is 11 km. Complete-time series data are needed for harmonics extraction. Transmitted waveform and spectrum are shown in Fig. 7, which mainly contains 39 main frequencies with large amplitude, 10 secondary frequencies with considerable amplitude, and a total of 49 candidate frequencies in this signal. This means that in one launch 49 frequencies are acquired at the same time, which are evenly distributed in the frequency domain. The survey signal is continuously transmitted in the distributed WFEM.

3.1.2 Working method in receiving terminal

As shown in Fig. 6, in traditional WFEM, it needs to observe 6 frequency groups of data,

and different signal receivers need to work simultaneously, while in distributed WFEM, receivers are independent with each other, and they do not need to work simultaneously. Since only one set of waveforms is needed, theoretically the total acquisition time is about 0.5 h for distributed WFEM, while the total acquisition time is about 2 h for traditional WFEM. In other words, in the case of the same acquisition time, the distributed WFEM greatly increases the number of superpositions of each frequency, which means that it is much easier to get data with a high signal-to-noise ratio for distributed WFEM.

Specifically, in actual exploration, it needs to set the shortest acquisition time in the target area, and dynamically adjust the acquisition time according to the noise situation in different areas.

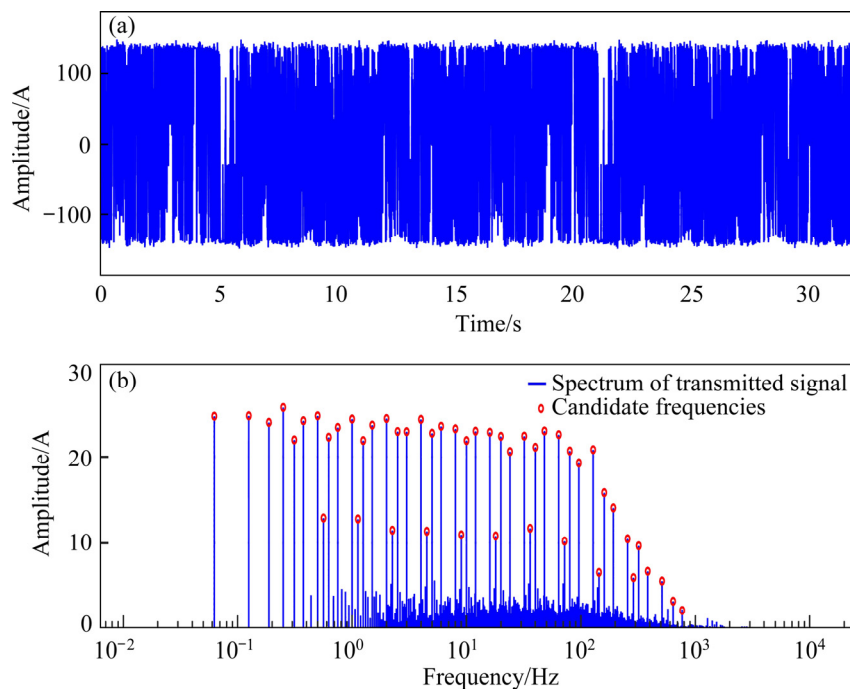


Fig. 7 Waveform (a) and spectrum (b) of real transmitted signal in Type L3-F39

In Litun Iron Mine, the signal is continuously transmitted. Different receiving groups are independent of each other and the rolling observations are carried out. The acquisition time for one single-point is set as 4096 s, and the sampling frequency is 25600 Hz, with the lowest frequency of 0.0625 Hz corresponding to 256 acquisition cycles, and the highest frequency of 768 Hz collecting 3145728 cycles in total. For each measuring point, there exists 104857600 sampling points, a huge data.

The waveforms and frequency spectra of real data at Point S150–420 are shown in Fig. 8. Although there is strong power frequency interference, as well as some communication interference, as shown in Fig. 8(c), benefitted from the long-term acquisition, it does not interfere much with target frequencies above 1 Hz and many frequencies are with the high signal-to-noise ratio. Low-frequency part is affected by electrode polarization and floating current. To solve this, a pre-processing based on Legendre polynomial is applied to eliminating part of low-frequency noise. The waveform and frequency spectrum after pre-processing are shown in Figs. 8(b, d), respectively. It is obvious that low-frequency noise is partially eliminated, and the spectrum of frequencies below 1 Hz is greatly improved.

As shown in Fig. 9, the normalized electric field curve of the measuring Point S150–420 is obtained by dividing electric field corresponding to each frequency obtained in Fig. 8(b) by the measured current in Fig. 7(b). Additionally, error bars are embedded for the normalized curve, from which it is clear that data obtained in Litun Iron Mine based on the distributed WFEM are of high quality in this area, especially in the middle and high frequency bands.

In Litun Iron Mine, with total of 20 receivers, each with 5 channels, using rolling measurement method, at most 400 measuring points of data collection were achieved in one day. A total of 1350 WFEM measuring points were completed in 4 d, with 338 measuring points per day on average. The efficiency of field work has been greatly improved.

3.2 Application result

In Litun Iron Mine, the WFEM inversion result is based on the one-dimensional finite element method [27,28]. Through the interpolation of different survey line data, the underground three-dimensional electrical data of the area are obtained. Take line S170 as an example to analyze the results of WFEM. As shown in Fig. 10, the stratum of line S170 is divided according to the electrical profile and a known borehole ZK1. The

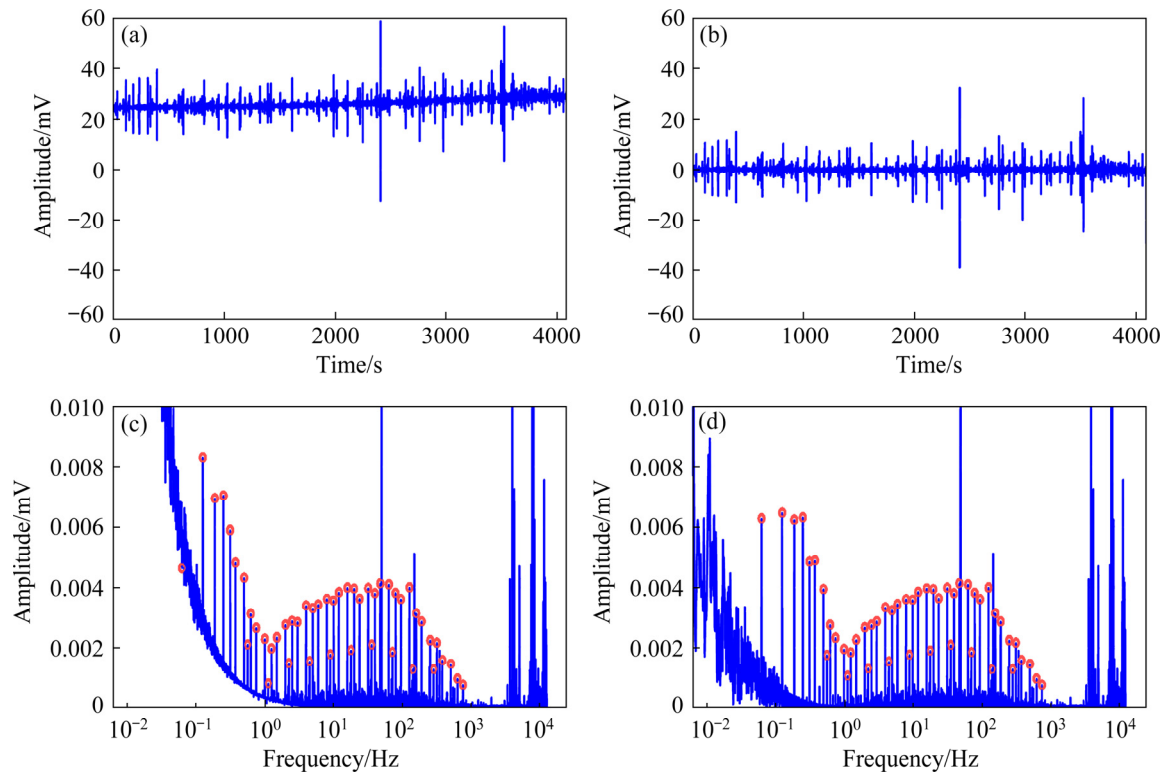


Fig. 8 Waveforms (a, b) and spectra (c, d) of raw data (a, c) and pre-processed data (b, d)

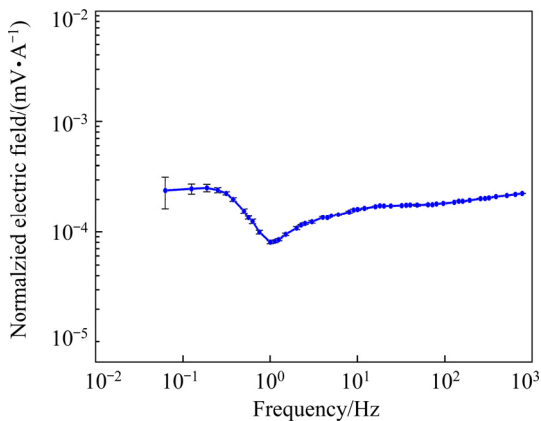


Fig. 9 Normalized electric field with error bars after pre-processing with 49 frequencies

Quaternary and Neogene strata in the survey line range from the shallow elevation of -1020 m, and the stratigraphic boundary is shallow in the east and deep in the west. The Carboniferous–Permian is shallow in the east and deep in the west within the survey line. Affected by intrusive rocks, the overall thickness in the east is relatively small, with a depth from -850 to -1300 m, and the depth in the west is below -1050 m. Diorite gradually thins from east to west, and the resistivity at the measuring Point 100–215 is generally low. It is inferred that at this time, the rocks below -2000 m are mainly

Carboniferous–Permian and Ordovician rocks. The borehole ZK1 is located at about 448 points of the survey line. The lithology of the borehole is shown in Fig. 10(b), in which the results of WFEM are consistent with known geological conditions.

Based on the inversion results of 23 survey lines in this survey area, three-dimensional electrical data shallower than 1800 m were obtained, as shown in Fig. 11(a). Based on the resistivity threshold, the Quaternary, Neogene strata, and underlying Carboniferous were picked up, as shown in Fig. 11(b), with 4 known boreholes with their lithology embedded. Also, in Fig. 11(b), the interface of the Permian strata and the underlying strata present the undulating shape of the intrusive rock mass.

Besides, there are two seismic survey lines Z1 and L1 crossing the survey area. The ore bodies in this area are covered with thick sedimentary strata, and the seismic exploration results reflect the stratum above the ore bodies well. Therefore, it can be used as a mutual verification with the results of distributed WFEM. The positions of the two seismic survey lines are shown in Fig. 12(a) and Fig. 13(a). Based on the three-dimensional electrical data, resistivity slices are obtained along

the direction of the two seismic survey lines separately.

As shown in Fig. 12(b), the stratum is divided according to the seismic exploration results of survey line Z1. According to the locations of the seismic survey line, the electrical slice of the corresponding position is obtained from the three-dimensional electrical data. The electrical slice is divided into three main electrical layers. The first layer is characterized by low resistivity, shallower than -900 m. It is the Quaternary and Neogene strata. The second layer presents the

characteristics of medium resistivity value. In the range from -900 to -1500 m in elevation, this layer is the Carboniferous–Permian. The third layer presents the characteristics of high resistivity, which is the deep diorite rock mass. The overall results of the WFEM inversion are consistent with the seismic profile, and the stratum buried depth is highly consistent.

According to the direction of the second seismic survey line L1, as shown in Fig. 13, the corresponding electrical profile is also obtained from the three-dimensional electrical data. And the

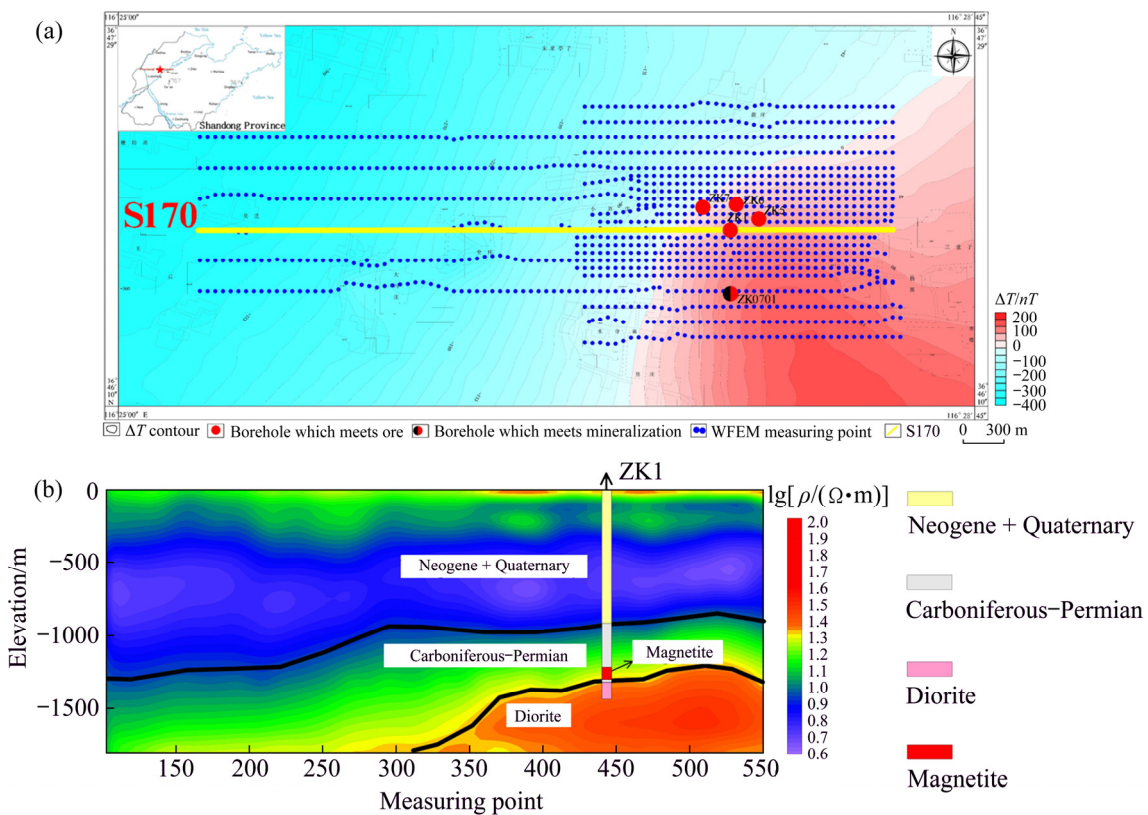


Fig. 10 Survey line S170 in survey area (a) and electrical profile and corresponding situation with known boreholes (b)

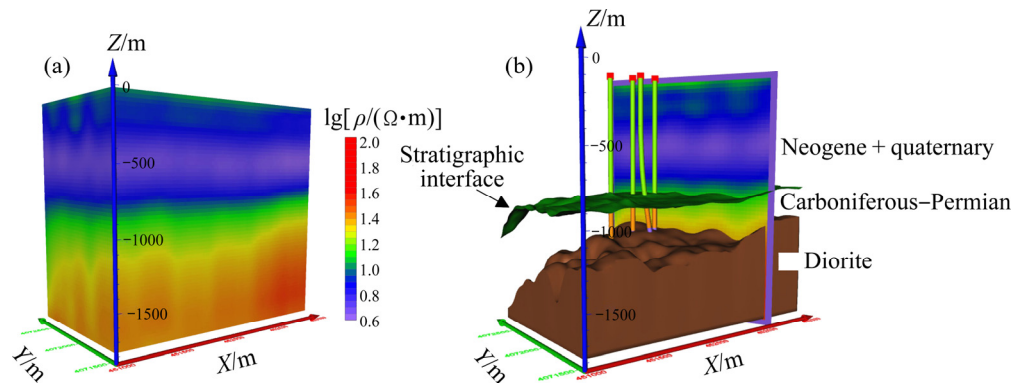


Fig. 11 Three-dimensional resistivity data (a) and three-dimensional electrical interfaces for different layers, longitudinal resistivity profile and borehole lithology embedded (b)

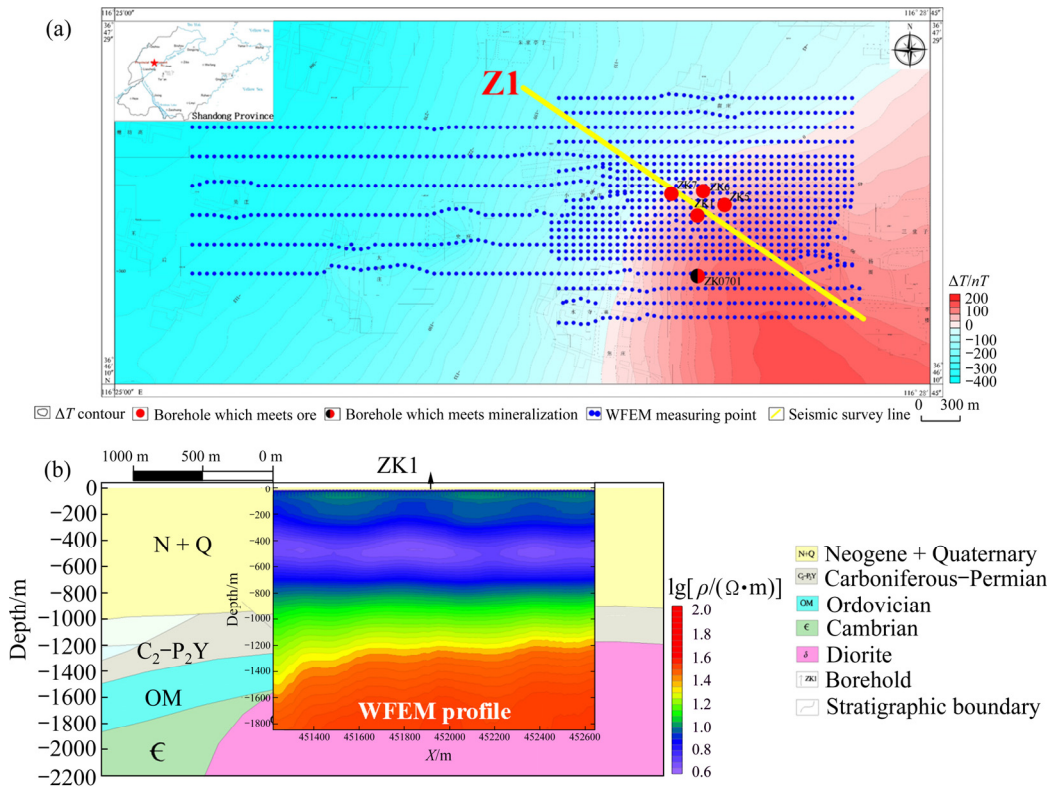


Fig. 12 Locations of seismic survey line Z1 (a) and comparison of distributed WFEM result and interpretation section based on seismic survey (b)

overall results of the distributed WFEM are consistent with the seismic profile, reflecting reliable exploration results.

It needs to be noted that the distributed WFEM survey did not directly discover the ore body in this area, but indirectly prospected through the description of the deep structure. There are many reasons for that, and the accuracy of the inversion is one of them. Therefore, in the future, the high-order pseudo-random signal in Type L6-F81 will be applied in this area, and expected to identify the ore body directly.

4 Conclusions

(1) Based on the 2ⁿ sequence pseudo-random signal, the high-order pseudo-random signal is proposed. By using this high-order pseudo-random signal, only one set of waveforms needs to be sent without changing the waveform or frequency, and the information for all target frequencies can be obtained at one time. Compared with the previous electromagnetic method, it greatly saves acquisition time. High-order pseudo-random signals, as same as 2ⁿ sequence pseudo-random signal, can be also

applied to other scenarios.

(2) In distributed WFM, the same waveform is continuously transmitted, while the receivers can acquire exploration signals at any time and at any location. Different receivers are independent of each other and can dynamically adjust the collection parameters according to the actual situation and interference. Once one of the receivers completes data acquisition, there is no need to wait for other receivers. Then, rolling acquisition is also realized in distributed WFEM, which doubles the exploration efficiency and greatly reduces the exploration cost.

(3) Benefitted from the high efficiency of distributed WFEM, more measuring points with massive complete series data are acquired in a short time. More frequencies, including both main frequencies and useful harmonics, are extracted at one time based on these massive data. More measuring points and more frequencies than before make large-scale and high-resolution three-dimensional distributed WFEM realizable. Thus, distributed WFEM can be applied to the fine exploration of deep resources, minerals, and others.

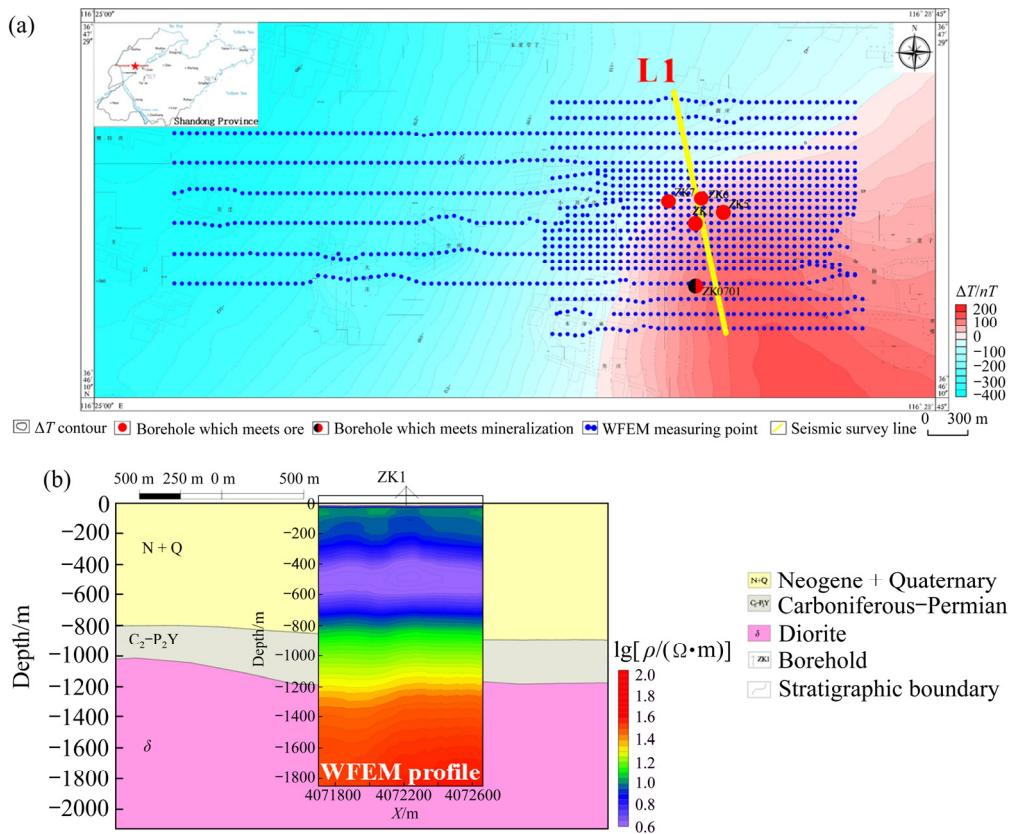


Fig. 13 Locations of seismic survey line L1 (a) and comparison of distributed WFEM result and interpretation section based on seismic survey (b)

Acknowledgments

This work is funded by the National Natural Science Foundation of China (No. 42004056), the Natural Science Foundation of Shandong Province, China (No. ZR2020QD052), and China Postdoctoral Science Foundation (No. 2019M652386).

References

- [1] HE Ji-shan. Theory and technology of wide field electromagnetic method [J]. Journal of the Non-ferrous Metal, 2019, 29(9): 1809–1816. (in Chinese)
- [2] HE Ji-shan. Wide field electromagnetic method and pseudo random signal method [M]. Beijing: Higher Education Press, 2010. (in Chinese)
- [3] HE Ji-Shan. Wide field electromagnetic sounding methods [J]. Journal of Central South University (Science and Technology), 2010, 41(3): 1065–1072.
- [4] TANG Jing-Tian, HE Ji-Shan. A new method to define the full-zone resistivity in horizontal electric dipole frequency soundings on a layered earth [J]. Acta Geophysica Sinica, 1994(7): 543–552.
- [5] HE Ji-shan, LIU Jian-xin. Pseudo-random multi-frequency phase method and its application [J]. The Chinese Journal of Nonferrous Metals, 2002, 12(2): 374–376. (in Chinese)
- [6] HE Ji-shan. Closed addition in a three-element set and 2ⁿ sequence pseudo-random signal coding [J]. Journal of Central South University (Science and Technology), 2010, 41(2): 632–637. (in Chinese)
- [7] HE Ji-shan, LI Di-quan, DAI Shi-kun. Shale gas detection with wide field electromagnetic method in North-western Hunan [J]. Oil Geophysical Prospecting, 2014, 49(5): 1006–1012. (in Chinese)
- [8] PENG Yong-hui, LI Di-quan. Study on electric structure in a hydrocarbon accumulation area, Qaidam Basin [J]. Lithologic Reservoirs, 2015, 27(1): 115–121. (in Chinese)
- [9] LING Fan, ZHU Yu-zhen, ZHOU Ming-lei, TIAN Hong-jun. Shale gas potential assessment of Changsan uplift area in southern North China basin by using wide field electromagnetic method [J]. Geophysical and Geochemical Exploration, 2017, 41(2): 369–376. (in Chinese)
- [10] HE Ji-shan. Combined application of wide-field electromagnetic method and flow field fitting method for high-resolution exploration: A case study of the Anjialing No. 1 coal mine [J]. Engineering, 2018, 4(5): 667–675.
- [11] HE Ji-Shan. New research progress in theory and application of wide field electromagnetic method [J]. Geophysical and Geochemical Exploration, 2020, 44(5): 985–990. (in Chinese)
- [12] TANG Jing-tian, REN Zheng-yong, ZHOU Cong, ZHANG Lin-cheng, YUAN Yuan. Frequency-domain electromagnetic methods for exploration of the shallow subsurface: A review

- [J]. Chinese Journal of Geophysics, 2015, 58(8): 2681–2705. (in Chinese)
- [13] CONSTABLE S, SRNKA J. An introduction to marine controlled-source electromagnetic methods for hydrocarbon exploration [J]. Geophysics, 2007, 72(2): WA3–WA12.
- [14] MYER D, CONSTABLE C S, KEY K. Broad-band waveforms and robust processing for marine CSEM surveys [J]. Geophysical Journal International, 2011, 184(2): 689–698.
- [15] ZIOLKOWSKI A, WRIGHT D, MATTSSON J. Comparison of pseudo-random binary sequence and square-wave transient controlled-source electromagnetic data over the peon gas discovery, Norway [J]. Geophysical Prospecting, 2011, 59(6): 1114–1131.
- [16] MITTET R, SCHAUGPETTERSEN T. Shaping optimal transmitter waveforms for marine CSEM surveys [J]. Geophysics, 2008, 73(3): F97–F104.
- [17] CONSTABLE S, COX C S. Marine controlled-source electromagnetic sounding: 2. The pegasus experiment [J]. Journal of Geophysical Research: Solid Earth, 1996, 101(B3): 5519–5530.
- [18] SRNKA L J, LU X. Logarithmic spectrum transmitter waveform for controlled-source electromagnetic surveying: US Patent, 7539279 [P]. 2009-05-26.
- [19] STRACK K M, HANSTEIN T H, EILENZ H N. LOTEM data processing for areas with high cultural noise levels [J]. Physics of the Earth and Planetary Interiors, 1989, 53(3/4): 261–269.
- [20] STREICH R, BECKEN M, RITTER O. Robust processing of noisy land-based controlled-source electromagnetic data [J]. Geophysics, 2013, 78(5): E237–E247.
- [21] MACLENNAN K, LI Yao-guo. Denoising multicomponent CSEM data with equivalent source processing techniques [J]. Geophysics, 2013, 78(3): E125–E135.
- [22] YANG Yang, LI Di-quan, TONG Tie-gang, ZHANG Dong, ZHOU Ya-tong, CHEN Yang-kang. Denoising controlled-source electromagnetic data using least-squares inversion [J]. Geophysics, 2018, 83(4): E229–E244.
- [23] YANG Yang, HE Ji-shan, LI Di-quan. A noise evaluation method for CSEM in the frequency-domain based on wavelet transform and analytic envelope [J]. Chinese Journal of Geophysics, 2018, 61(1): 344–357. (in Chinese)
- [24] YANG Yang, HE Ji-shan, LI Di-quan. Energy distribution and effective components analysis of 2^n sequence pseudo-random signal [J]. Transactions of Nonferrous Metals Society of China, 2021, 31(7): 2102–2115.
- [25] HE Ji-shan, YANG Yang, LI Di-quan, WENG Jing-bo. Method and system for generating high-order pseudo-random electromagnetic prospecting signal: CN Patent, 2020103447332 [P]. 2020–08–11.
- [26] BRACEWELL R N. The Fourier transform & its applications [M]. WCB/McGraw Hill, 2000.
- [27] YU Yun-chun. One-dimensional forward and inversion for wide field electromagnetic method [D]. Changsha: Central South University, 2010. (in Chinese)
- [28] WANNAMAKER P E, STODT J A, RIJO L. A stable finite element solution for two-dimensional magnetotelluric modeling [J]. Geophysical Journal International, 1987, 88: 277–296.

基于高阶 2^n 序列伪随机信号的分布式广域电磁法

杨洋¹, 何继善^{2,3}, 凌帆^{2,3}, 朱裕振^{1,4}

1. 山东大学 岩土与结构工程研究中心, 济南 250061;
2. 香港中文大学(深圳) 城市地下空间及能源研究院, 深圳 518172;
3. 中南大学 地球科学与信息物理学院, 长沙 410083;
4. 山东省煤田地质规划勘察研究院, 济南 250109

摘要: 为实现三维电磁探测, 提出一种基于高阶 2^n 序列伪随机信号的分布式广域电磁探测方法。该方法在勘探时只需要发射一组高阶伪随机波形, 即可获得所有目标探测频率。发射波形可以根据勘探任务定制; 采集终端独立接收信号, 能够根据实际情况对采集参数动态调整。在齐河-禹城深部富铁矿的野外勘探试验表明, 分布式广域电磁法能够实现短时间海量电磁数据的高效获取。与传统电磁勘探方法相比, 基于高阶伪随机信号的分布式广域电磁法野外勘探效率更高。该方法能够应用于深部资源与矿产的大规模精细探测。

关键词: 分布式广域电磁法; 高阶伪随机信号; 多频; 海量数据

(Edited by Bing YANG)